

Effect of the organic functionalization of flexible MOFs on the adsorption of CO₂†

Thomas Devic,^{*a} Fabrice Salles,^b Sandrine Bourrelly,^c Béatrice Moulin,^d Guillaume Maurin,^b Patricia Horcajada,^a Christian Serre,^a Alexandre Vimont,^d Jean-Claude Lavalley,^d Hervé Leclerc,^d Guillaume Clet,^d Marco Daturi,^d Phillip L. Llewellyn,^c Yaroslav Filinchuk‡^e and Gérard Férey^a

Received 15th November 2011, Accepted 18th January 2012

DOI: 10.1039/c2jm15887f

The adsorption of CO₂ by a series of functionalized flexible MIL-53(Fe) solids has been evaluated through a combination of *in situ* X-ray power diffraction, adsorption calorimetry, IR spectroscopy and computer modelling. It appears that (i) strongly polar groups maintain the nonporous structure in its closed form due to strong intra-framework interactions and (ii) less polar functional groups allow only a modulation of the CO₂-framework interactions, in some cases with a disappearance of the initial intra-framework μ₂-OH...X hydrogen bonds, but do not interact directly with the CO₂ molecules.

Introduction

Metal Organic Frameworks (MOFs) are considered as promising materials for the storage and separation of fluids.¹ In the case of gases, the capture of CO₂ from various mixtures using MOFs as adsorbents, either through Vacuum or Pressure Swing Adsorption (VSA/PSA) processes or *via* the use of membranes appears appealing (ref. 2–5 and references therein). Indeed, compared to other porous solids, advantages of MOFs lie in their higher pore surface and/or their accessible metal sites, but also in their easily tuneable pore surface (through organic functionalization) and sometimes structural flexibility (adaptation of the pore size and shape to its content). The last two items, either together or separately, have been considered to modulate or improve the adsorption of CO₂ in MOFs. Functionalization indeed appears as a rather easy method to improve the selectivity by the introduction of groups (such as amines) that may interact strongly with CO₂,^{6–15} characterization of the adsorbate/adsorbent interactions by *in situ* infrared spectroscopy, measurement of the

adsorption enthalpy by microcalorimetry or localization of the adsorbates by X-ray diffraction being the ultimate proof of efficiency. Adsorption of CO₂ in flexible MOFs is characterized by the appearance of steps in the adsorption isotherms, associated with changes in the crystal structure and the pore opening.^{16–24} *In situ* techniques have been coupled with molecular simulation to show that a critical strength of the host-guest interactions is required for inducing the switching from one structural form to the other.²⁵ Indeed, for such solids, the organic functionalization also impacts the flexible character of the framework and the general shape of the adsorption isotherms. Finally, when moving from pure gas (CO₂) to mixtures (CO₂/CH₄, CO₂/N₂,...), either under static (co-adsorption isotherms) or dynamic (breakthrough curves) conditions, the behaviour of the flexible solids becomes even more complex, the main issue being that the pore opening, the selectivity and the composition of the gas phase are intimately interdependent.^{26–30}

Here, we will focus on the single gas CO₂ adsorption in a series of flexible functionalized iron based MOFs. These compounds belong to the MIL-53 type,³¹ a family of trivalent metal (M^{III}) (M = Cr, Fe, Al, Ga, In, Sc) terephthalates built up from chains of μ₂-OH corner-sharing MO₆ octahedra linked to each other by the organic ligands to define diamond-shaped 1-D pores (Fig. 1a).

In this series, the pore opening of the activated (empty pores) at room temperature form depends on the nature of the metal, whereas an orthorhombic large pore (LP) form associated with a permanent porosity is present for M = Al, Cr,³¹ a monoclinic closed pore (CP) form is observed for M = Fe (see Fig. 2 top).³² Nevertheless, all the solids are flexible upon adsorption of polar^{20,33} or apolar^{34–37} gases, vapours or liquids and exhibit steps in the adsorption isotherms associated either with a decrease or an increase of the pore volume ('breathing' or 'swelling' behaviour). MIL-53(Cr, Al) in the presence of CO₂ exhibits a flexible

^aInstitut Lavoisier, UMR CNRS 8180, Université de Versailles Saint-Quentin-en-Yvelines, 45 avenue des Etats-Unis, 78035 Versailles cedex, France. E-mail: devic@chimie.uvsq.fr

^bInstitut Charles Gerhardt Montpellier, UMR CNRS 5253, UM2, ENSCM, Place E. Bataillon, 34095 Montpellier cedex 05, France

^cLaboratoire Chimie Provence, UMR 6264, Universités Aix-Marseille I, II & III—CNRS, Centre de Saint Jérôme, 13397 Marseille Cedex 2, France

^dLaboratoire Catalyse et Spectrochimie, ENSICAEN, Université de Caen, CNRS, 6 Bd Maréchal Juin, 14050 Caen, France

^eSwiss Norwegian Beam Lines at ESRF, 38043 Grenoble, France

† Electronic supplementary information (ESI) available: *In situ* PXRD patterns under CO₂ pressure, isotherms and enthalpies of adsorption, details about the DFT calculations and IR studies on the activated solids. See DOI: 10.1039/c2jm15887f

‡ Current address: Institute of Condensed Matter and Nanosciences, Université catholique de Louvain, Place L. Pasteur 1, 1348 Louvain-la-Neuve, Belgium.

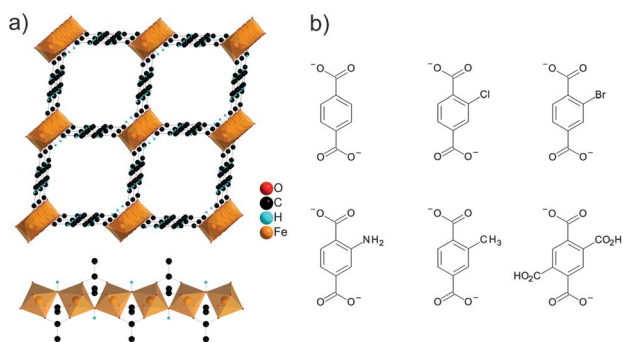


Fig. 1 (a) Crystal structure of MIL-53(Fe): (top) in the LP form, (bottom) the inorganic chain; (b) functionalized terephthalate linkers considered in the present study.

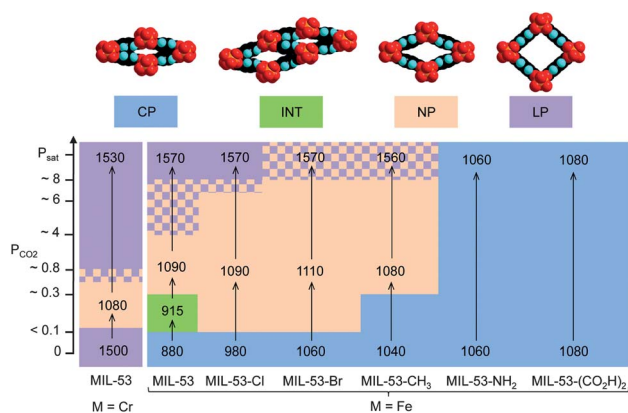


Fig. 2 Schematic representation of the results of the *in situ* XRPD experiments. Top: pore openings in the MIL-53 system (CP: closed pore, INT: intermediate triclinic, NP: narrow pore, LP: large pore); bottom: evolution of the pore opening and unit cell volume with the CO₂ pressure at 230 K for the MIL-53(Cr) and MIL-53(Fe)-X solids.

character, evolving from a LP to a monoclinic narrow pore (NP) and finally to a LP form when an increasing amount of CO₂ is adsorbed (see Fig. 2),^{20,22} the first step (LP → NP) being related to the strong donor–acceptor interactions occurring between the μ₂-OH groups and the CO₂ molecules.^{20,38–40} In contrast, these solids remain rigid (LP form) at room temperature upon adsorption of CH₄.²² In the case of CO₂/CH₄ mixtures in MIL-53(Cr), the flexible character depends on the CO₂/CH₄ ratio, but the NP form was shown to adsorb CO₂ exclusively, leading to high CO₂/CH₄ selectivity when this form is predominant (*i.e.* in a certain range of pressure and composition).²⁷ In the case of MIL-53(Al), the functionalization with NH₂ group was shown to enhance this selectivity.^{26,29,41,42} Interestingly, it was recently emphasized that such a modification is not related to the expected additional NH₂⋯CO₂ interaction but rather to a modulation of the breathing behaviour.⁴³ Other polar groups (OH, NO₂) seem also to have a beneficial effect on the capacity of adsorption at low pressure for MIL-53(Al), but the relation between these results and the breathing behaviour was not studied.⁴⁴ We recently reported a series of modified MIL-53(Fe) solids bearing functional groups of various polarity and

hydrophilicity (see Fig. 1).^{45–47} We showed that their dispersion in various liquids leads to a selective pore opening, which depends on the liquid/grafted function pair.⁴⁶ Adsorption of linear alkanes in MIL-53(Fe)-Cl, -Br and -CH₃ was also very recently investigated.⁴⁸ All solids present a flexible behaviour, and compared to the parent MIL-53(Fe), slight improvements were detected, in terms of (i) capacity (at least at low pressure) and (ii) kinetics of adsorption, especially for the longest alkane molecules.⁴⁸ Both effects were attributed to a higher degree of initial pore opening of the modified MIL-53(Fe) solids in the empty (CP) form, which depends on the whole on the steric hindrance of the functional group.

In the present work, we studied the adsorption of CO₂ in a series of MIL-53(Fe)-X solids (X = Cl, Br, CH₃, NH₂, (CO₂H)₂, see Fig. 1b) in comparison with the parent non-functionalized solid.⁴⁹ Their adsorptive properties were first screened by *in situ* X-ray Powder Diffraction (XRPD). The solids which were found to present significant structural changes upon adsorption were then studied in depth by a combination of techniques (adsorption gravimetry, microcalorimetry, *in situ* infrared (IR) spectroscopy and molecular simulations) in order to gain a deeper understanding of the effect of the functional group towards adsorption both at the macroscopic and microscopic levels.

Experimental section

Synthesis

The MIL-53(Fe)-X solids (X = —, Cl, Br, CH₃, NH₂, (CO₂H)₂) were synthesized and activated following the published procedures.^{32,46}

In situ XRPD studies

XRPD patterns under gas pressure were collected at the BM01A station at the Swiss Norwegian Beam Line of the European Synchrotron Radiation Facility (ESRF, Grenoble, France). The powdered samples were introduced in a 1 mm quartz capillary and connected to a home-made gas dosing system.³⁴ Prior to the experiments, the samples were outgassed under vacuum (pressure of about 10⁻³ mbar) at 473 K for a few hours. The temperature was then adjusted to 230 K, and doses of CO₂ were introduced. XRPD were collected using a MAR345 imaging plate with a sample-to-detector distance of 300–400 mm (depending on the experiment, λ = 0.809264, 0.694018 or 0.7183 Å). X-Ray powder diffractograms were collected one minute after the gas introduction, with an acquisition time of 30 to 60 seconds (rotation rate 1° s⁻¹). New XRPD patterns were recorded at the same pressure every five minutes, and equilibrium (at a given pressure) was assumed when no change was observed between the successive patterns. The data were integrated using the Fit2D program (Dr A. Hammersley, ESRF) and a calibration measurement of a NIST LaB₆ standard sample. The patterns were indexed using the Dicvol software,⁵⁰ Le Bail fits were then performed with the Fullprof2k software package⁵¹ *via* the Winplotr interface.⁵² The resulting unit-cell parameters are summarized in Table 1.

Table 1 Cell parameters of the MIL-53(Cr) and the MIL-53(Fe)-X solids (X = —, Cl, Br, CH₃, NH₂, (CO₂H)₂) upon different CO₂ pressures at 230 K

Solid	P_{CO_2} /bar	Space group	$a/\text{\AA}$	$b/\text{\AA}$	$c/\text{\AA}$	$\alpha/^\circ$	$\beta/^\circ$	$\gamma/^\circ$	$V/\text{\AA}^3$	Form
MIL-53(Cr)	0	<i>Imcm</i>	16.7628(4)	13.1113(3)	6.8336(1)	90	90	90	1501.91(6)	LP
	0.25	<i>C2/c</i>	19.680(2)	8.4067(6)	6.8024(5)	90	105.987(7)	90	1081.9(1)	NP
	8.7	<i>Imcm</i>	16.3456(3)	13.6719(3)	6.8498(1)	90	90	90	1530.75(5)	LP
MIL-53(Fe) ⁴⁶	0	<i>C2/c</i>	21.356(2)	6.6138(6)	6.8756(7)	90	115.23(1)(6)	90	878.5(1)	CP
	0.82	<i>P1</i>	6.8773(6)	10.600(1)	13.919(2)	111.01(1)	87.21(1)	104.75(1)	915.0(2)	INT
	1.10	<i>C2/c</i>	19.7895(5)	8.2672(2)	6.8790(2)	90	105.280(3)	90	1085.64(5)	NP
	7.84	<i>Imcm</i>	16.556(5)	13.6991(5)	6.9198(2)	90	90	90	1569.10(8)	LP
	0	<i>C2/c</i> or <i>Ce</i>	20.1084(4)	7.3258(2)	6.9043(1)	90	105.624(2)	90	979.50(4)	CP
MIL-53(Fe)-Cl	1.5	<i>C2/c</i> or <i>Ce</i>	20.1736(3)	8.1805(1)	6.9004(1)	90	107.270(1)	90	1087.43(3)	NP
	8.7	<i>Imcm</i>	16.7135(1)	13.5452(1)	6.94039(5)	90	90	90	1571.22(2)	LP
	0	<i>C2/c</i> or <i>Ce</i>	20.145(1)	7.4408(8)	6.9140(5)	90	105.975(6)	90	996.5(1)	CP
MIL-53(Fe)-Cl ^a	42.1	<i>C2/c</i> or <i>Ce</i>	20.1856(8)	8.3248(3)	6.9123(3)	90	107.543(4)	90	1107.6(1)	NP
	0	<i>C2/c</i> or <i>Ce</i>	20.1733(6)	7.9512(3)	6.9141(2)	90	106.839(2)	90	1061.43(5)	CP
MIL-53(Fe)-Br	1.7	<i>C2/c</i> or <i>Ce</i>	20.2912(5)	8.3257(2)	6.9270(1)	90	108.122(2)	90	1111.76(5)	NP
	10.7	<i>C2/c</i> or <i>Ce</i>	20.315(1)	8.3727(4)	6.9271(3)	90	108.192(4)	90	1119.36(8)	NP ^b
	0	<i>Imcm</i>	16.605(2)	13.627(1)	6.9276(6)	90	90	90	1567.5(2)	LP ^b
MIL-53(Fe)-CH ₃	0	<i>C2/c</i> or <i>Ce</i>	20.002(2)	7.8738(9)	6.8804(6)	90	106.059(8)	90	1041.3(2)	CP
	7.0	<i>C2/c</i> or <i>Ce</i>	20.059(2)	8.1544(7)	6.8928(6)	90	106.88(1)	90	1078.9(2)	NP
	10.0	<i>C2/c</i> or <i>Ce</i>	20.055(2)	8.1642(6)	6.9119(8)	90	107.05(1)	90	1082.0(2)	NP ^b
MIL-53(Fe)-NH ₂	0	<i>Imcm</i>	16.589(2)	13.531(1)	6.9343(5)	90	90	90	1556.5(3)	LP ^b
	0	<i>C2/c</i> or <i>Ce</i>	20.151(2)	7.8482(7)	6.9730(5)	90	106.459(7)	90	1057.6(1)	CP
	11.9	<i>C2/c</i> or <i>Ce</i>	20.152(2)	7.8515(7)	6.9751(5)	90	106.492(7)	90	1058.2(1)	CP
MIL-53(Fe)-(CO ₂ H) ₂	0	<i>C2/c</i> or <i>Ce</i>	20.0303(2)	8.0451(1)	6.9637(1)	90	106.405(1)	90	1076.48(2)	CP
	11.0	<i>C2/c</i> or <i>Ce</i>	20.0337(2)	8.0421(1)	6.9624(1)	90	106.403(1)	90	1076.08(2)	CP

^a Collected at 303 K. ^b Mixture of the two forms. CP: closed pore, INT: intermediate triclinic, NP: narrow pore, LP: large pore.

Adsorption gravimetry and microcalorimetry

Approximately 0.5 g of sample was used for each adsorption experiment. Prior to each analysis, the sample was outgassed at 473 K for 16 hours under vacuum. The gravimetric adsorption experiments were carried out at 303 K and at pressures up to 50–60 bar using a commercial gravimetric adsorption device (Rubotherm Präzisionsmeßtechnik GmbH).⁵³ A step by step gas introduction mode was used. Equilibrium was assumed when the variation of weight remained below 0.03% for 20 minutes. In this apparatus the variation in sample weight and gas density can be measured consequently. The latter is obtained using a titanium sinker of known mass and volume and thus allows a direct correction of the buoyancy effect. The enthalpies of adsorption were obtained *via* a manometric adsorption apparatus coupled with a Tian–Calvet type microcalorimeter.⁵⁴ A point by point introduction adsorptive procedure was used to evaluate the amounts adsorbed and a pseudo-differential enthalpy of adsorption *via* the measured exothermic thermal effect associated with each dose.

In situ IR spectroscopy

The solid was deposited on a silicon wafer after dispersion in ethanol. The mixture was dried in air and placed in an IR quartz cell equipped with KBr windows. A movable quartz sample holder allowed positioning of the sample in the infrared beam for IR measurements or into the furnace for thermal treatments. The cell is connected to a vacuum line for evacuation, calcination and introduction of doses of vapours or gases. All spectra were recorded at room temperature. Before adsorption of CO₂, the compounds were pretreated under vacuum at 473 K for one hour. Transmission spectra were recorded in the 500–5600 cm⁻¹ range at 4 cm⁻¹ resolution on a Nicolet Nexus spectrometer

equipped with an extended KBr beam splitting device and a mercury cadmium telluride (MCT) cryodetector. CO₂ was purified by freeze thawing before use.

Molecular simulation

Starting with the experimental unit cell parameters provided in Table 1, the initial models for the NP forms of the modified MIL-53(Fe)-X (X = Cl, Br, CH₃) present at 230 K upon CO₂ adsorption were built up using the same computationally assisted structure determination strategy that we previously validated on different MOFs (see ESI† for more details).⁴⁶ The so-obtained structure models were further geometry optimized by density functional theory (DFT) calculations in the absence and in the presence of either 1 or 2 CO₂ molecules per pore. The latter loading corresponds to conditions where the saturation limit for CO₂ inside the NP form is reached. The CO₂ molecules were first inserted by chemical intuition based on the conclusions previously drawn for the non-modified MIL-53(Cr).^{20,38,39} These starting geometries include single interactions between either the oxygen or the carbon of the CO₂ and the hydrogen or oxygen of the μ_2 -OH group respectively and a double interaction where a CO₂ molecule bridges μ_2 -OH groups on opposing walls. These DFT calculations were performed using the PW91 GGA density functional and the double numerical basis set containing polarization functions on hydrogen atoms (DNP) as implemented in DMol³ code.⁵⁵ To speed up the convergence, both the smearing (at 0.005 Ha) option for the orbital occupancy and semi-core pseudo-potentials were employed.

Complementary grand canonical Monte Carlo simulations based on generic forcefields and partial charges for the host frameworks (see details in the ESI†) have been performed to determine the adsorption enthalpy at low coverage for CO₂ in the

NP forms of all the investigated MIL-53(Fe)-X (X = —, Cl, Br, CH₃).

Results and discussion

In their dried state, all the solids present a CP form, whose unit cell volume depends on the nature and number of grafted functions (see Table 1). Nevertheless, none of the selected solids exhibit any accessible porosity relative to nitrogen at 77 K.⁴⁶ Significant adsorption of CO₂ thus requires a pore opening, which should be easily detected by X-ray diffraction. In this prospect, the MIL-53(Fe)-X (X = —, Cl, Br, CH₃, NH₂, (CO₂H)₂) solids were subjected to *in situ* XRPD analysis at 230 K under variable pressure of CO₂ (from 0 to $P_{\text{sat}} \approx 9$ bar), as well as MIL-53(Cr) for comparison. The resulting patterns for MIL-53(Fe)-Cl and MIL-53(Fe)-NH₂ are shown in Fig. 3 (see Fig. S1† for the other solids). All patterns were indexed and subjected to a Le Bail refinement, the final unit-cell parameters are summarized in Table 1. Taking into account the symmetry and the pore volume, all the patterns can be ascribed to structural forms already defined for the pristine MIL-53(Cr, Fe) materials. Depending on the metal M (M = Cr, Fe) and functional group X,

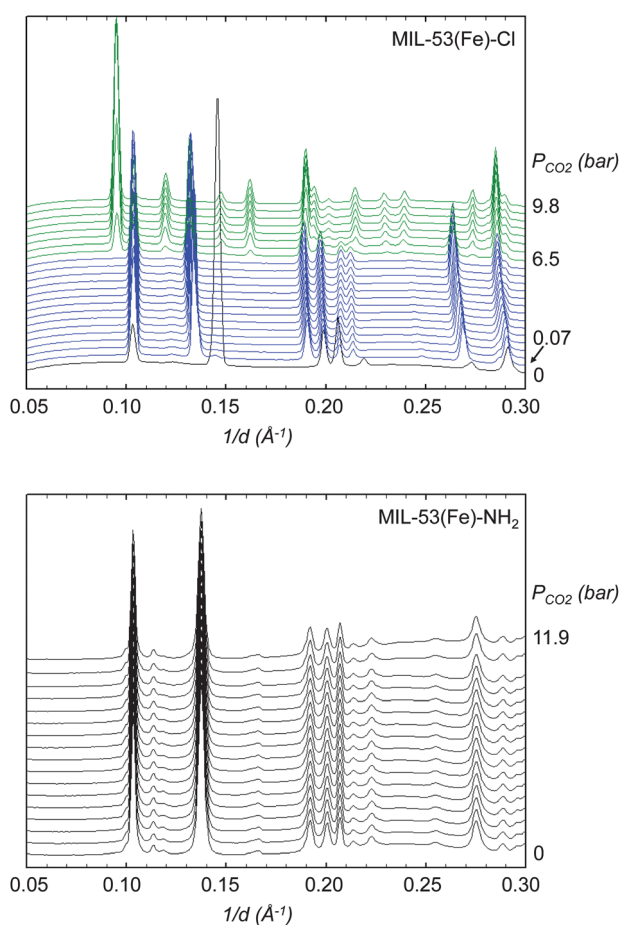


Fig. 3 Adsorption of CO₂ on MIL-53(Fe)-Cl (top) and MIL-53(Fe)-NH₂ (bottom) at 230 K followed by XRPD. The colour corresponds to the major phase observed at the given pressure. Black: anhydrous CP form; blue: NP form, green: LP form (see ESI† for other solids).

various behaviours were observed, which are summarized in Fig. 2.

MIL-53(Cr) undergoes the already reported LP to NP and NP to LP transitions,²⁰ with a downshift of the transition pressures related to the change of temperature (here 230 K vs. 293 K in ref. 20). In contrast, MIL-53(Fe) behaves differently,⁴⁹ with three structural transitions corresponding to a stepwise opening of the pores (from CP to an intermediate triclinic form (INT) to NP and finally to LP, see Fig. 3), in accordance with the behaviour previously reported for water desorption³² and alkane adsorption.³⁴

From a qualitative point of view, the MIL-53(Fe)-X solids can be divided into two groups.

(i) The ones belonging to the first family (X = Cl, Br, CH₃) present a two step behaviour, with a first slight pore opening at low pressure (CP → NP transition), followed by the appearance of a LP version at higher pressure, which was observed to be pure only for X = Cl. These solids thus present a direct transition from the CP to the NP form, whereas the parent MIL-53(Fe) exhibits an intermediate triclinic state labelled as INT, in which only half of the pores are slightly opened while the others remain closed. This phenomenon was already observed upon adsorption of alkanes, and has been attributed to the bulkiness of the substituents, which prevents the coexistence of two pore apertures in a unique crystalline phase.⁴⁸ The reversibility of the transformation was confirmed for MIL-53(Fe)-Cl, but was associated with a hysteresis ($P_{\text{NP} \rightarrow \text{LP}} > P_{\text{LP} \rightarrow \text{NP}}$, see Fig. S2†), as already observed for MIL-53(Cr).^{20,22} Finally, whereas the full transformation from CP to NP and further to LP is observed at 230 K between 0 and 10 bar, only the first step (CP to NP) transition is detected at 303 K in the pressure range available (0–42 bar, see Fig. S3†). This is in agreement with a shift of the steps to higher pressure when the temperature increases, once again in agreement with our previous findings for MIL-53(Cr)^{22,56} (see above).

(ii) The other two MIL-53(Fe)-X solids (X = NH₂, (CO₂H)₂) present a peculiar behaviour, as they both remain rigid and nonporous (in the CP form) on the whole pressure range. This result could appear astonishing at a first sight, as these functional groups were expected to interact strongly with CO₂.^{57,58} Nevertheless, it can be understood in light of the intra-framework attractive interactions (interactions between linkers or between linkers and μ_2 -OH groups) evidenced in our previous work.⁴⁶ These interactions need to be overcome by the CO₂...framework interactions in order to allow the opening of the pores. For X = (CO₂H)₂, the presence of strong X...X hydrogen bonds in the CP form was unambiguously established by single crystal XRD,⁴⁷ and explains the fact that this solid remains in the CP form, even when dispersed in polar liquids such as water or ethanol.⁴⁶ The same phenomenon is here in play with CO₂. Similarly, it was shown that the functionalization by X = NH₂ tends to stabilize the CP form in MIL-53(Al), a phenomenon which was also attributed to the formation of intra-framework NH₂...O hydrogen bonds.^{41,43} Both the nature of the metal (Fe) and the grafted function (NH₂) thus favour the stabilization of the CP form, leading to the absence of pore opening upon CO₂ pressure for MIL-53(Fe)-NH₂.

Based on these results, only the solids which present structural changes (X = —, Cl, Br, CH₃) upon CO₂ adsorption were subsequently explored for determining their adsorption

performances at 303 K, both at low pressure (0–2 bar, coupled with microcalorimetry) and high pressure (up to 50 bar). Data are shown in Fig. 4 together with MIL-53(Cr) for comparison. In order to get rid of the effect of the functional group on the molar mass, isotherms are reported in mol mol⁻¹ rather than in the commonly used mmol g⁻¹ unit (see Fig. S5† for this unit).

As already reported, the isotherm of MIL-53(Cr) presents a step, associated with the appearance of the NP form at intermediate pressure, while the solid is in a LP form at both low and high pressures.^{20,22} At first sight, only the non-modified MIL-53(Fe) solid presents a comparable flexible behaviour but with two visible steps (CP → INT and INT → NP), whereas the others behave as rigid solids with type I isotherms. Indeed, even at low pressure, no step on the isotherm could be detected for MIL-53(Fe)-X (X = —, Cl, Br, CH₃). This is nevertheless in agreement with the *in situ* XRPD data, which showed (for MIL-53(Fe)-Cl) at 303 K, after a first CP to NP transition at low pressure, only the NP form up to at least 42 bar (Fig. S3†). Consequently, the associated isotherm presents only one plateau. This is supported by the analysis of the adsorbed amount of CO₂ (see below). Using as a reference the case of MIL-53(Cr), the NP and LP forms are expected to adsorb at saturation about 0.7 and

2.2 mol mol⁻¹, respectively. For MIL-53(Fe), the second plateau (between 5 and 40 bar, $n_{\text{ads}} \approx 0.8$ mol mol⁻¹) is thus associated with the filling of the NP form, whereas the first one at lower pressure (<5 bar) is assigned to adsorption occurring in the INT form with a capacity half of the one for the NP form (0.35 mol mol⁻¹).³⁴ The LP form does not appear on the pressure range studied. Further, all the functionalized solids present a similar plateau at 0.5 mol mol⁻¹, corresponding to a lower adsorption capacity than the pristine MIL-53(Cr, Fe) materials *in the same* NP form. This can be understood in light of the micropore volumes for both types of solids. These are summarized in Table 2, evaluated from the simulated NP structures for each modified MIL-53(Fe) using the procedure reported by Dürren *et al.*⁵⁹ The resulting micropore volumes are significantly lower for all the functionalized MIL-53(Fe)-X than for the parent solid. They also compare well with the ones extracted from the CO₂ isotherms (Table 2, see ESI† for details about the calculations). This reveals that the steric hindrance of the functional group affects the capacity of the NP form, either by directly blocking the access of the pore or by inducing the rotation of the phenyl cores that restricts the space available for guest molecules.

As detailed earlier, the objective of functional groups is to tune (in most cases enhance) the CO₂···framework (possibly X) interactions. Adsorption enthalpies can give information on the strongest adsorption sites for the adsorbate molecules, and thus discriminate the MIL-53(Fe)-X solids. Here, similar values at low coverage are observed (between -45 and -38 kJ mol⁻¹), with the order -Br < -CH₃ ≈ -Cl (see Fig. S4†), in agreement with simulated values (Table S2†). Note that the adsorption enthalpy was shown to depend on the pore opening,²² and that the pristine MIL-53(Fe) can thus not be directly compared to the modified solids, as the sequence of pore opening differs. The aforementioned order is consistent with the slopes of the isotherms at low pressure (Fig. 4), and indicates that CO₂ has a higher affinity for MIL-53(Fe)-Br than MIL-53(Fe)-CH₃ and finally MIL-53(Fe)-Cl. In order to determine if this different energetic behaviour results from a stronger CO₂···framework interaction or is a consequence of a confinement effect, *in situ* IR measurements and DFT simulations were realized on the NP forms of MIL-53(Fe)-X (X = —, Cl, Br, CH₃). DFT calculations were further able to define the preferential arrangements of the CO₂ within the porosity of these modified MIL-53(Fe) NP forms.

It has been previously shown that infrared spectroscopy was able to precisely characterize the bridged μ₂-OH group of the functionalized MIL-53(Fe)s.⁴⁶ In its activated form, MIL-53(Fe)-CH₃ exhibits unique ν(OH) and δ(OH) bands, indicating the presence of hydroxyl groups in a single environment, free of any interaction, while MIL-53(Fe)-Cl and -Br present two

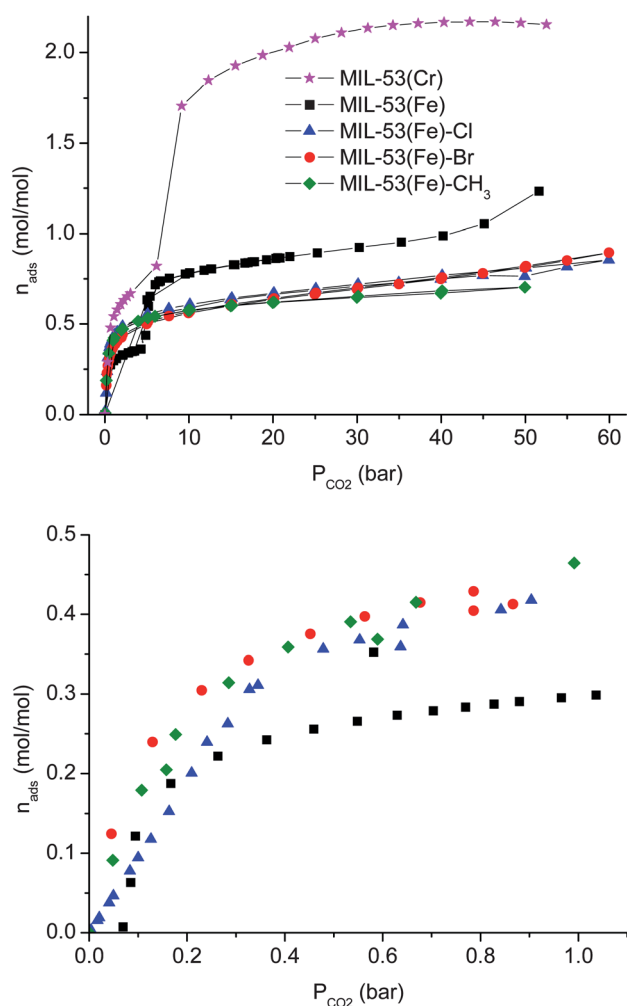


Fig. 4 Adsorption isotherms of CO₂ on MIL-53(Fe)-X (X = —, Cl, Br, CH₃) at 303 K. Top: high pressure range; bottom: low pressure range.

Table 2 Comparison of micropore volumes extracted from the CO₂ adsorption isotherms and from the simulated crystal structures

Solid	Form	V isotherm/ cm ³ g ⁻¹	V simulated/ cm ³ g ⁻¹
MIL-53(Fe)	INT	0.11	0.11
	NP	0.31	0.31
MIL-53(Fe)-Cl	NP	0.23	0.26
MIL-53(Fe)-Br	NP	0.21	0.21
MIL-53(Fe)-CH ₃	NP	0.21	0.23

$\nu(\text{OH})$ and two $\delta(\text{OH})$ bands, assigned to the presence of hydroxyl groups both free of any interaction (OH_{free}) and hydrogen bonded to the halogen group (OH_{X}) (Fig. 5). This interaction appears stronger for MIL-53(Fe)-Br than for MIL-53(Fe)-Cl. All these observations are in full agreement with the conclusions drawn from DFT simulations, especially the distribution of the Mulliken charges (Table S2†) which indicates stronger electrostatic interactions between X and the $\mu_2\text{-OH}$ groups in MIL-53(Fe)-Br than in MIL-53(Fe)-Cl (see ref. 46 and ESI† for details).

Adsorption of CO_2 in the MIL-53(Fe)-X solids was then followed by IR spectroscopy (Fig. 5). In all cases, it leads to the perturbation of the bands associated with the $\mu_2\text{-OH}$ group, as already evidenced for MIL-53(Cr).^{20,40} For MIL-53(Fe)- CH_3 , both the $\nu(\text{OH})$ and $\delta(\text{OH})$ bands are shifted (from 3649 to 3621 cm^{-1} , $\Delta\nu(\text{OH}) = 28 \text{ cm}^{-1}$ and from 842 to 881 cm^{-1} , $\Delta\delta(\text{OH}) = 39 \text{ cm}^{-1}$) and the ν_2 band of the adsorbed CO_2 is split into two components (651 and 661 cm^{-1}). The shift of the $\nu(\text{OH})$ and $\delta(\text{OH})$ bands can be interpreted as the result of the formation of a hydrogen bond between the O atom of the CO_2 molecule and the H atom of the $\mu_2\text{-OH}$ group. This is confirmed by the DFT optimized geometry for CO_2 in the NP form of the MIL-53(Fe)- CH_3 (Fig. 6b) which shows characteristic $\text{O}(\text{CO}_2)\cdots\text{H}(\mu_2\text{-OH})$ distances ranging from 2.27 to 2.60 Å. This interaction is comparable to that observed in the case of MIL-53(Cr)^{20,40} but is much weaker than the one observed with silica ($\Delta\nu(\text{OH}) = 58 \text{ cm}^{-1}$),⁶⁰ in agreement with the higher acidity of the silanol group of silica. The splitting of the $\nu_2(\text{CO}_2)$ band indicates a supplementary donor-acceptor interaction, for which the C atom acts as an electron acceptor center, the electron-donor center being either the O atom of the hydroxyl or the carboxylate groups.⁴⁰ From the DFT optimized geometry (Fig. 6b), one observes that

the C atom of the CO_2 molecule interacts preferentially with the O atom of the carboxylate group, the $\text{C}(\text{CO}_2)\cdots\text{O}(\text{carboxylate})$ distances of 2.81 Å being significantly shorter than the $\text{C}(\text{CO}_2)\cdots\text{O}(\mu_2\text{-OH})$ ones (above 3.4 Å). This behaviour differs from what is predicted for the non-modified MIL-53(Fe) (Fig. 6a) where the carbon atom of the CO_2 molecule interacts more preferentially with the oxygen atom of the hydroxyl group of the chain, with a $\text{C}(\text{CO}_2)\cdots\text{O}(\mu_2\text{-OH})$ distance of about 3.10 Å, consistent with our previous findings for the NP forms of the MIL-53(Cr, Al).^{20,38} This deviation can be explained by the different orientations of the CO_2 molecules within the pores, the presence of the CH_3 group constraining the CO_2 molecules to be more lined up along the direction of the tunnel, while they remain nearly parallel to each other in the same way as in the non-modified version. In the case of MIL-53(Fe)-Br and -Cl, the adsorption of CO_2 gives rise to the same interactions with the hydroxyl groups free of any interaction prior to adsorption (OH_{free}) (see Fig. 5). The case of the hydrogen bonded groups (OH_{X}) is more ambiguous, as in the $\nu(\text{OH})$ range, its signal (at 3621 cm^{-1}) at least partially overlaps with the OH_{free} band perturbed by the interaction with CO_2 (3620 cm^{-1} for MIL-53(Fe)-Cl and 3592 cm^{-1} for MIL-53(Fe)-Br), precluding any deep interpretation. Nevertheless, information can be extracted in the $\delta(\text{OH})$ range. The inset in Fig. 5 presents the spectra of the solids after adsorption of CO_2 (at 0.2 bars) subtracted from the ones before adsorption. The negative band at about 850 cm^{-1} reflects the fraction of OH_{free} involved in the interaction with CO_2 , characterized by a positive band at 890 cm^{-1} . For MIL-53(Fe)-Cl and -Br, the negative band is asymmetric toward higher wavenumber, suggesting that a few OH_{X} groups also interact with CO_2 . Finally, the presence of a single perturbed $\delta(\text{OH})$ band (890 cm^{-1}) suggests that the interaction of CO_2 with OH_{X} and OH_{free} are identical. This implies that the interaction of CO_2 with OH_{X} breaks the $\mu_2\text{-OH}\cdots\text{X}$ hydrogen bond. This phenomenon was further confirmed by DFT calculations. Indeed, compared to the situation in the CP form, one observes that the CO_2 molecules tend to break the intra-framework $\mu_2\text{-OH}\cdots\text{X}$ hydrogen bonds, mainly due to a reorientation of the $\mu_2\text{-OH}$ group for optimizing the interactions with the guest molecules. Indeed, while the characteristic $\mu_2\text{-OH}\cdots\text{X}$ distances are of 2.4 and 2.5 Å for -Cl and -Br forms respectively in the empty CP form, here in the presence of CO_2 these distances become significantly longer of about 3.5 and 3.25 Å. This behavior comes from the orientation change of the hydroxyl group when interacting with CO_2 , as demonstrated by comparing the Fe-O-H angle, which varies by approximately 10% between the optimized CO_2 -loaded NP and empty CP simulated structures. The CO_2 thus adopts a geometry that favors relatively strong interactions between both their carbon and oxygen atoms with the oxygen and the hydrogen of the $\mu_2\text{-OH}$ groups respectively (Fig. 6c and d). Such an arrangement is comparable to the one obtained for the parent MIL-53(Fe) (Fig. 6a) and MIL-53(Cr)²⁰ in their NP forms. We further observe relatively weak interactions between CO_2 and the functional groups, the characteristic distances separating these two species being above 3.2 Å (Fig. 6b-d). This result emphasizes that in these MIL-53(Fe) materials, the functionalization does not provide an expected additional $\text{X}\cdots\text{CO}_2$ interaction but rather a modulation of the interaction with the preferential $\mu_2\text{-OH}$ adsorption sites while the contraction of the structure is not

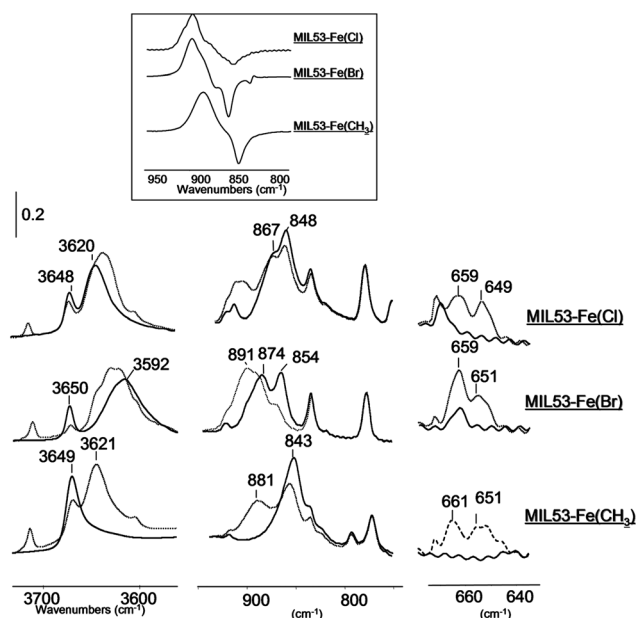


Fig. 5 Spectra of MIL-53(Fe) samples activated at 473 K before (full line) and after introduction of 0.2 bar of CO_2 at room temperature (dashed line) (a) MIL-53(Fe)- CH_3 , (b) MIL-53(Fe)-Br, (c) MIL-53(Fe)-Cl. Inset: subtracted spectra in the $\delta(\text{OH})$ range of structural hydroxyl groups.

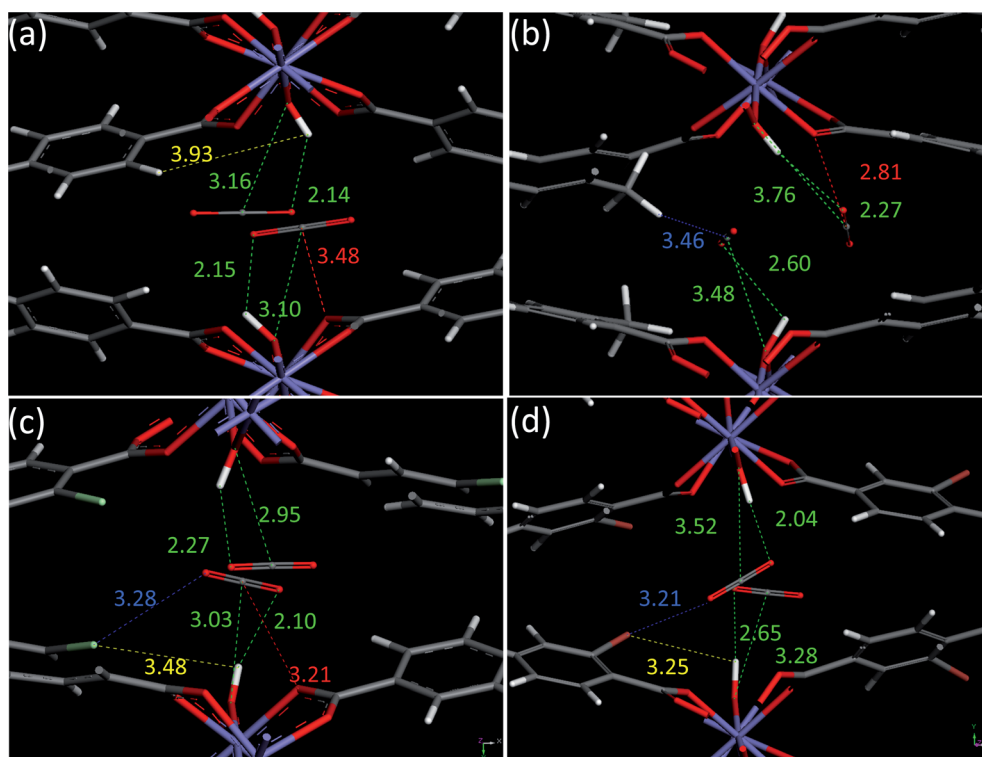


Fig. 6 Arrangement of the CO₂ molecules in the NP forms for MIL-53(Fe)-X (X = — (a), CH₃ (b), Cl (c) and Br (d)) at 2 CO₂/pore, obtained from DFT calculations. The distances are reported for CO₂...μ₂-OH (in green), μ₂-OH...X (in yellow), CO₂-O(carboxylate) (in red) and CO₂-X (blue).

affected. This indirect impact of the functionalization is complementary to what has been previously reported for the MIL-53(Al)-NH₂ where the amino group induced a change of the breathing behaviour.⁴³

Finally, all these results can be compared with previous studies associated with other series of functionalized MOFs.⁵ In the case of rigid solids, it was shown both theoretically (for example on the UiO-66 (ref. 58) and IRMOF⁶¹ series) and experimentally (on ZIF,¹¹ IRMOF¹⁵ and DMOF⁹ series) that polar groups (such as Br, NO₂, CN, OH, and SO₃H) tend to strengthen the CO₂-framework interaction at low pressure (leading to higher enthalpy of adsorption and capacity) and thus increase the selectivity towards less polar gases, although they lead to a reduction of the pore volume at high pressure. For the MIL-53-X series (X other than NH₂ (ref. 26,41 and 42)), both theoretical⁵⁷ and experimental⁴⁴ work did not tackle the flexible character, but the present study suggests that the 'positive' effect of polar groups tend to be hidden by intra-framework effects. This confirms once again that reasoning on host-guest interactions is meaningful only when these interactions are able to overcome the framework-framework attraction. This 'third' effect should be taken into account whatever series of flexible MOFs and guests are considered.

Conclusions

The adsorption of CO₂ in a series of flexible solids of the MIL-53(Fe) type was investigated by a multi-technique approach. The solids bearing functional groups which could potentially lead to strong interactions with CO₂ (CO₂H, NH₂)⁵⁸ were found to

remain in their nonporous CP forms under the investigated conditions, because of strong intra-framework interactions favouring the pore closure. In contrast, the MIL-53(Fe)-X (X = Cl, Br, CH₃) solids adsorb a significant amount of CO₂ with a flexible character (CP → NP and NP → LP transitions). These functional groups do not directly interact with the CO₂ molecules, but allow modulation of the interactions between the guest molecules and the inorganic μ₂-OH groups as suggested by microcalorimetry. Nevertheless, this interaction is associated for X = Cl and Br with the disappearance of the intra-framework μ₂-OH...X hydrogen bonds, highlighting the complex interplay between framework-framework and guest-framework interactions in the adsorption processes.

Acknowledgements

The authors acknowledge the financial support of the French ANR 'NOMAC' (ANR-06-CO₂-008) and the UE through the FP6-STREP 'DeSANNS' (SES6-020133). The ESRF is acknowledged for providing access to the Swiss-Norwegian Beam Line.

Notes and references

- 1 See the special issue: *Chem. Soc. Rev.*, 2009, **38**, and references therein.
- 2 S. Keskin, T. M. van Heest and D. S. Sholl, *ChemSusChem*, 2010, **3**, 879–891.
- 3 J.-R. Li, R. J. Kuppler and H. C. Zhou, *Chem. Soc. Rev.*, 2009, **38**, 1477–1504.
- 4 J.-R. Li, Y. Ma, M. C. McCarthy, J. Sculley, J. Yu, H.-K. Jeong, P. B. Balbuena and H.-C. Zhou, *Coord. Chem. Rev.*, 2011, **255**, 1791–1823.

- 5 K. Sumida, D. L. Rogow, J. A. Mason, T. M. McDonald, E. D. Bloch, Z. R. Herm, T.-H. Bae and J. R. Long, *Chem. Rev.*, 2012, **112**, 724–781.
- 6 Z. Chen, S. Xiang, H. D. Arman, P. Li, D. Zhao and B. Chen, *Eur. J. Inorg. Chem.*, 2011, 2227–2231.
- 7 T. Panda, P. Pachfule, Y. Chen, J. Jiang and R. Banerjee, *Chem. Commun.*, 2011, **47**, 2011–2013.
- 8 X. Si, C. Jiao, F. Li, J. Zhang, S. Wang, S. Liu, Z. Li, L. Sun, F. Xu, Z. Gabelica and C. Schick, *Energy Environ. Sci.*, 2011, **4**, 4522–4527.
- 9 Y. Zhao, H. Wu, T. J. Emge, Q. Gong, N. Nijem, Y. J. Chabal, L. Kong, D. C. Langreth, H. Liu, H. Zeng and J. Li, *Chem.–Eur. J.*, 2011, **17**, 5101–5109.
- 10 B. Zheng, J. Bai, J. Duan, L. Wojtas and M. J. Zaworotko, *J. Am. Chem. Soc.*, 2011, **133**, 748–751.
- 11 R. Banerjee, H. Furukawa, D. Britt, C. Knobler, M. O'Keeffe and O. M. Yaghi, *J. Am. Chem. Soc.*, 2009, **131**, 3875–3877.
- 12 R. Vaidhyanathan, S. S. Iremonger, G. K. H. Shimizu, P. G. Boyd, S. Alavi and T. K. Woo, *Science*, 2010, **330**, 650–653.
- 13 A. Demessence, D. M. D'Alessandro, M. L. Foo and J. R. Long, *J. Am. Chem. Soc.*, 2009, **131**, 8784–8786.
- 14 J. P. S. Mowat, S. R. Miller, J. M. Griffin, V. R. Seymour, S. E. Ashbrook, S. P. Thompson, D. Fairen-Jimenez, A.-M. Banu, T. Düren and P. A. Wright, *Inorg. Chem.*, 2011, **50**, 10844–10858.
- 15 H. Deng, C. J. Doonan, H. Furukawa, R. B. Ferreira, J. Towne, C. B. Knobler, B. Wang and O. M. Yaghi, *Science*, 2010, **327**, 846–850.
- 16 A. Kondo, H. Noguchi, S. Ohnishi, H. Kajiro, A. Tohdoh, Y. Hattori, W. C. Xu, H. Tanaka, H. Kanoh and K. Kaneko, *Nano Lett.*, 2006, **6**, 2581–2584.
- 17 H.-S. Choi and M. P. Suh, *Angew. Chem., Int. Ed.*, 2009, **48**, 6865–6869.
- 18 S. Takamizawa, Y. Takasaki and R. Miyake, *Chem. Commun.*, 2009, 6625–6627.
- 19 J. Zhang, H. Wu, T. J. Emge and J. Li, *Chem. Commun.*, 2010, **46**, 9152–9154.
- 20 C. Serre, S. Bourrelly, A. Vimont, N. A. Ramsahye, G. Maurin, P. L. Llewellyn, M. Daturi, Y. Filinchuk, O. Leynaud, B. Barnes and G. Férey, *Adv. Mater.*, 2007, **19**, 2246–2251.
- 21 R. Kitaura, K. Seki, G. Akiyama and S. Kitagawa, *Angew. Chem., Int. Ed.*, 2003, **42**, 428–431.
- 22 S. Bourrelly, P. L. Llewellyn, C. Serre, F. Millange, T. Loiseau and G. Férey, *J. Am. Chem. Soc.*, 2005, **127**, 13519–13521.
- 23 S. Galli, N. Masciocchi, G. Tagliabue, A. Sironi, J. A. R. Navarro, J. M. Salas, L. Mendez-Liñan, M. Domingo, M. Perez-Mendoza and E. Barea, *Chem.–Eur. J.*, 2008, **14**, 9890–9901.
- 24 H. Leclerc, T. Devic, S. Devautour-Vinot, P. Bazin, N. Audebrand, G. Férey, M. Daturi, A. Vimont and G. Clet, *J. Phys. Chem. C*, 2011, **115**, 19828–19840.
- 25 G. Férey, C. Serre, T. Devic, G. Maurin, H. Jobic, P. L. Llewellyn, G. De Weireld, A. Vimont, M. Daturi and J.-S. Chang, *Chem. Soc. Rev.*, 2011, **40**, 550–562.
- 26 S. Couck, J. F. M. Denayer, G. V. Baron, T. Rémy, J. Gascon and F. Kapteijn, *J. Am. Chem. Soc.*, 2009, **131**, 6326–6327.
- 27 L. Hamon, P. L. Llewellyn, T. Devic, A. Ghoufi, G. Clet, V. Guillerme, G. D. Pirngruber, G. Maurin, C. Serre, G. Driver, W. van Beek, E. Jolimaître, A. Vimont, M. Daturi and G. Férey, *J. Am. Chem. Soc.*, 2009, **131**, 17490–17499.
- 28 Y. Inubushi, S. Horike, T. Fukushima, G. Akiyama, R. Matsuda and S. Kitagawa, *Chem. Commun.*, 2010, **46**, 9229–9231.
- 29 V. Finsy, L. Ma, L. Alaerts, D. E. De Vos, G. V. Baron and J. F. M. Denayer, *Microporous Mesoporous Mater.*, 2009, **120**, 221–227.
- 30 E. Barea, G. Tagliabue, W.-G. Wang, M. Pérez-Mendoza, L. Mendez-Liñan, F. J. López-Garzon, S. Galli, N. Masciocchi and J. A. R. Navarro, *Chem.–Eur. J.*, 2010, **16**, 931–937.
- 31 C. Serre, F. Millange, C. Thouvenot, M. Nogués, G. Marsolier, D. Louer and G. Férey, *J. Am. Chem. Soc.*, 2002, **124**, 13519–13526.
- 32 F. Millange, N. Guillou, R. I. Walton, J.-M. Grenèche, I. Margiolaki and G. Férey, *Chem. Commun.*, 2008, 4732–4734.
- 33 S. Bourrelly, B. A. Moulin, A. Rivera, G. Maurin, S. Devautour-Vinot, C. Serre, T. Devic, P. Horcajada, A. Vimont, G. Clet, M. Daturi, J.-C. Lavalley, S. Loera-Serna, R. Denoyel, P. L. Llewellyn and G. Férey, *J. Am. Chem. Soc.*, 2010, **132**, 9488–9498.
- 34 P. L. Llewellyn, P. Horcajada, G. Maurin, T. Devic, N. Rosenbach, S. Bourrelly, C. Serre, D. Vincent, S. Loera-Serna, Y. Filinchuk and G. Férey, *J. Am. Chem. Soc.*, 2009, **131**, 13002–13008.
- 35 P. L. Llewellyn, G. Maurin, T. Devic, S. Loera-Serna, N. Rosenbach, C. Serre, S. Bourrelly, P. Horcajada, Y. Filinchuk and G. Férey, *J. Am. Chem. Soc.*, 2008, **130**, 12808–12814.
- 36 L. Alaerts, M. Maes, L. Giebler, P. A. Jacobs, J. A. Martens, J. F. M. Denayer, C. E. A. Kirschhock and D. E. De Vos, *J. Am. Chem. Soc.*, 2008, **130**, 14170–14178.
- 37 V. Finsy, C. E. A. Kirschhock, G. Vedts, M. Maes, L. Alaerts, D. E. De Vos, G. V. Baron and J. F. M. Denayer, *Chem.–Eur. J.*, 2009, **15**, 7724–7731.
- 38 N. A. Ramsahye, G. Maurin, S. Bourrelly, P. L. Llewellyn, T. Loiseau, C. Serre and G. Férey, *Chem. Commun.*, 2007, 3261–3263.
- 39 N. A. Ramsahye, G. Maurin, S. Bourrelly, P. L. Llewellyn, C. Serre, T. Loiseau, T. Devic and G. Férey, *J. Phys. Chem. C*, 2008, **112**, 514–520.
- 40 A. Vimont, A. Travert, P. Bazin, J.-C. Lavalley, M. Daturi, C. Serre, G. Férey, S. Bourrelly and P. L. Llewellyn, *Chem. Commun.*, 2007, 3291–3293.
- 41 A. Boutin, S. Couck, F.-X. Coudert, P. Serra-Crespo, J. Gascon, F. Kapteijn, A. H. Fuchs and J. F. M. Denayer, *Microporous Mesoporous Mater.*, 2011, **140**, 108–113.
- 42 T. Lescouet, E. Kockrick, G. Bergeret, M. Pera-Titus and D. Farrusseng, *Dalton Trans.*, 2011, **40**, 11359–11361.
- 43 E. Stavitski, E. A. Pidko, S. Couck, T. Remy, E. J. M. Hensen, B. M. Weckhuysen, J. Denayer, J. Gascon and F. Kapteijn, *Langmuir*, 2011, **27**, 3970–3976.
- 44 S. Biswas, T. Ahnfeldt and N. Stock, *Inorg. Chem.*, 2011, **50**, 9518–9526.
- 45 S. Bauer, C. Serre, T. Devic, P. Horcajada, J. Marrot, G. Férey and N. Stock, *Inorg. Chem.*, 2008, **47**, 7568–7576.
- 46 T. Devic, P. Horcajada, C. Serre, F. Salles, G. Maurin, B. A. Moulin, D. Heurtaux, G. Clet, A. Vimont, J.-M. Grenèche, B. L. Ouay, F. Moreau, E. Magnier, Y. Filinchuk, J. Marrot, J.-C. Lavalley, M. Daturi and G. Férey, *J. Am. Chem. Soc.*, 2010, **132**, 1127–1136.
- 47 M. Sanselme, J.-M. Grenèche, M. Riou-Cavellec and G. Férey, *Solid State Sci.*, 2004, **6**, 853–858.
- 48 N. A. Ramsahye, T. K. Trung, S. Bourrelly, Q. Yang, T. Devic, G. Maurin, P. Horcajada, P. L. Llewellyn, P. Yot, C. Serre, Y. Filinchuk, F. Fajula, G. Férey and P. Trens, *J. Phys. Chem. C*, 2011, **115**, 18683–18695.
- 49 N. Guillou, F. Millange, R. I. Walton and P. L. Llewellyn, manuscript in preparation.
- 50 A. Boulitif and D. Louër, *J. Appl. Crystallogr.*, 2004, **37**, 724.
- 51 T. Roisnel and J. Rodriguez-Carjaval, in *7th European Powder Diffraction Conference*, ed. R. Delhez and E. J. Mittemeijer, Trans Tech Publications Ltd, Zurich-Uetikon, Barcelona, Spain, 2001, p. 118.
- 52 J. Rodriguez-Carjaval, <http://www.ill.eu/sites/fullprof/index.html>.
- 53 G. De Weireld, M. Frère and R. Jadot, *Meas. Sci. Technol.*, 1999, **10**, 117–126.
- 54 P. L. Llewellyn and G. Maurin, *C. R. Chim.*, 2005, **8**, 283–302.
- 55 *DMOL³*, v. Accelrys, Inc, San Diego, 2010.
- 56 F. Salles, H. Jobic, A. Ghoufi, P. L. Llewellyn, C. Serre, S. Bourrelly, G. Férey and G. Maurin, *Angew. Chem., Int. Ed.*, 2009, **48**, 8335–8339.
- 57 A. Torrisi, R. G. Bell and C. Mellot-Draznieks, *Cryst. Growth Des.*, 2010, **10**, 2839–2841.
- 58 Q. Yang, A. D. Wiersum, P. L. Llewellyn, V. Guillerme, C. Serre and G. Maurin, *Chem. Commun.*, 2011, **47**, 9603–9605.
- 59 T. Düren, F. Millange, G. Férey, K. S. Walton and R. Q. Snurr, *J. Phys. Chem. C*, 2007, **111**, 15350–15356.
- 60 A. Vimont, unpublished results.
- 61 W. Mu, D. Liu, Q. Yang and C. Zhong, *Microporous Mesoporous Mater.*, 2010, **130**, 76–82.